Solvothermal Synthesis and Characterization of Chalcopyrite CuInSe$_2$ Nanoparticles

Huiyu Chen · Seong-Man Yu · Dong-Wook Shin · Ji-Beom Yoo

Abstract The ternary I-III-VI$_2$ semiconductor of CuInSe$_2$ nanoparticles with controllable size was synthesized via a simple solvothermal method by the reaction of elemental selenium powder and CuCl as well as InCl$_3$ directly in the presence of anhydrous ethylenediamine as solvent. X-ray diffraction patterns and scanning electron microscopy characterization confirmed that CuInSe$_2$ nanoparticles with high purity were obtained at different temperatures by varying solvothermal time, and the optimal temperature for preparing CuInSe$_2$ nanoparticles was found to be between 180 and 220 °C. Indium selenide was detected as the intermediate state at the initial stage during the formation of pure ternary compound, and the formation of copper-related binary phase was completely deterred in that the more stable complex [Cu(C$_2$H$_8$N$_2$)$_2$]$^+$ was produced by the strong N-chelation of ethylenediamine with Cu$^+$. These CuInSe$_2$ nanoparticles possess a band gap of 1.05 eV calculated from UV–vis spectrum, and maybe can be applicable to the solar cell devices.

Keywords CuInSe$_2$ · Nanoparticles · Solvothermal method · Characterization · Solar cells

H. Chen · J.-B. Yoo
School of Advanced Materials Science & Engineering (BK21),
Sungkyunkwan University, Suwon 440-746, Republic of Korea

S.-M. Yu · D.-W. Shin · J.-B. Yoo (✉)
SKKU Advanced Institute of Nanotechnology (SAINT),
Sungkyunkwan University, Suwon 440-746, Republic of Korea
e-mail: jbyoo@skku.edu

Introduction

The development of new energy resources has been of great interest to materials scientists in recent years, because the traditional fossil fuels were gradually exhausted. Many efforts have been focused on renewable energy materials including photovoltaic electric generators. Among them, the ternary I-III-VI$_2$ semiconductor of CuInSe$_2$ has drawn much attention and becomes a candidate as a promising material for solar cell applications on account of its high optical absorption coefficient, low band gap ($\sim$ 1.05 eV), and good radiation stability [1–4]. Until now, several methods were employed to fabricate CuInSe$_2$, such as sputtering [5], evaporation [6], electrodeposition [7, 8], and pyrolysis of molecular single-source precursors [9]. However, most of these techniques usually require either special equipments or high processing temperature, and some of them use environment-unfriendly reagents such as organometallic compounds or H$_2$Se. There are only a few reports so far about the synthesis of CuInSe$_2$ nanostructures using solution-based approaches, partly due to their complexity of synthetic process and difficulty in controlling the pure phase. Typically, CuInSe$_2$ nanorods with diameter of 50–100 nm were prepared in ethylenediamine using Se powder, In$_2$Se$_3$, and CuCl$_2$ anhydrous powder as the starting materials [10]. Xie et al. reported the solvothermal synthesis of CuInSe$_2$ nanowhiskers and nanorods by using structure-directing organic amine solvents [11, 12]. More recently, CuInSe$_2$ nanoparticles were successfully synthesized in oleylamine solvent [13–15], and nanorings and nanocrystals with trigonal pyramidal shape were also prepared via the similar route [16, 17]. Furthermore, Li's group developed a facile synthesis and morphology control of CuInSe$_2$ nanocrystals using alkanethiol as ligand

and octadecene as noncoordinating solvent at a relatively low temperature [18].

It is well known that the physical and chemical properties of nanoscale materials strongly depend on their size, size distribution, and defect structure [19]. Also considering the construction of solar cells with high efficiency and low cost from colloidal semiconductor nanoparticles is one of the hottest topics in nanoparticle research, thus, developing a facile method to fabricate $CuInSe_2$ with controllable size is the prerequisite for any of their further applications. Herein, we report a solvothermal synthesis of $CuInSe_2$ nanoparticles with controllable size in anhydrous ethylenediamine solvent and no additional surfactants were employed. Some important factors such as reaction time, temperature, and concentrations of starting materials were systematically investigated in details.

Experimental Details

All chemicals were used as received without further purification. Elemental selenium powder (99.5 + %), copper (I) chloride (> 99.0%), and indium (III) chloride (99.99%) were purchased from Aldrich Chemical Co., anhydrous ethylenediamine was obtained from Kanto Chemical Co., Inc, Japan. In a typical experimental procedure, elemental Se powder (0.237 g, 3 mmol) was dissolved in 40-mL anhydrous ethylenediamine with magnetic stirring for 2 h, then CuCl (0.15 g, 1.5 mmol) and $InCl_3$ (0.332 g, 1.5 mmol) were added. The earlier mentioned mixture was continuously stirred for 2 h and then was loaded into a Teflon-lined stainless steel autoclave of 55 mL capacity. The autoclave was sealed and maintained at 200 °C for 24 h in an electric oven. After the reaction, the autoclave was allowed to cool naturally to room temperature and the nanoparticles existed in ethylenediamine solution with black color were collected by centrifugation, rinsed with distilled water and absolute ethanol several times to remove the by-products. Finally, the pure product was obtained and stored in absolute ethanol at room temperature. Other controlled experiments were carried out in details by changing the reaction time, temperature, and concentrations of starting materials.

The phase and crystallinity of the as-prepared samples were characterized by X-ray diffraction (XRD) on a Bruker D8 Discover diffractometer equipped with Cu Kα ($\lambda = 0.15406$ nm) radiation in the 2θ range from 20 to 80° while the voltage and electric current were held at 40 kV and 40 mA, respectively. Scanning electron microscopy (SEM) images were obtained using a JEOL JSM7401F field emission scanning electron microscope. Transmission electron microscopy (TEM) image, high-resolution TEM (HRTEM) image, and the corresponding selected area electron diffraction (SAED) pattern were taken on a JEOL JEM3010 transmission electron microscope with an accelerating voltage of 300 kV. X-ray photoelectron spectroscopy (XPS) measurements were carried out on an ESCA 2000 spectrometer using an Al Kα X-ray as the excitation source. Raman spectrum were measured from 50 to 350 cm^{-1} at room temperature using the 514-nm line of an Ar$^+$ laser beam with a power level of 30 mW (RM1000-Invia, Renishaw). The UV–vis absorption spectrum of the obtained product was recorded using a UV–vis–NIR spectrophotometer (SHIMADZU, UV-3600).

Results and Discussion

In order to synthesize the ternary compounds $CuInSe_2$ with high purity, the amounts of the starting precursors should be complied with their stoichiometry because otherwise additional second phases such as Cu_2Se, CuSe, or In_2Se_3 would be introduced on the basis of phase diagram [20]. Therefore, we employed all the precursors with their stoichiometric ratio during the synthetic procedure. The phase structure and purity of the $CuInSe_2$ product obtained at 200 °C for 24 h were examined by X-ray diffraction (XRD). As shown in Fig. 1a, all the diffraction peaks in the XRD pattern can be indexed to pure phase of $CuInSe_2$ with chalcopyrite tetragonal structure, and the lattice constants

Fig. 1 XRD pattern (**a**) and Raman spectrum (**b**) of $CuInSe_2$ product prepared at 200 °C for 24 h
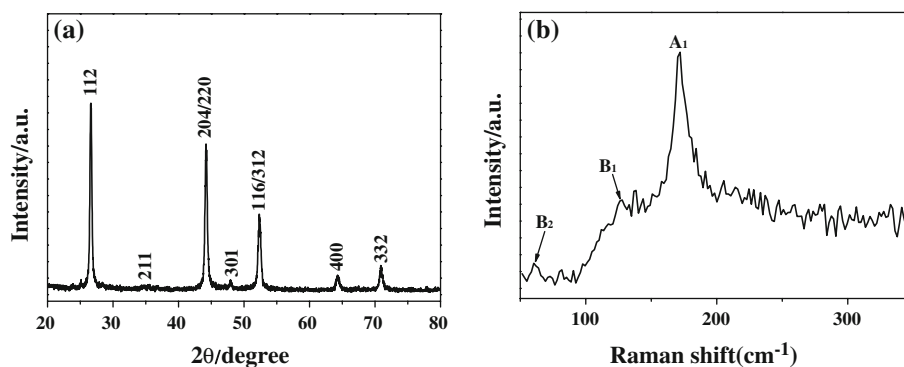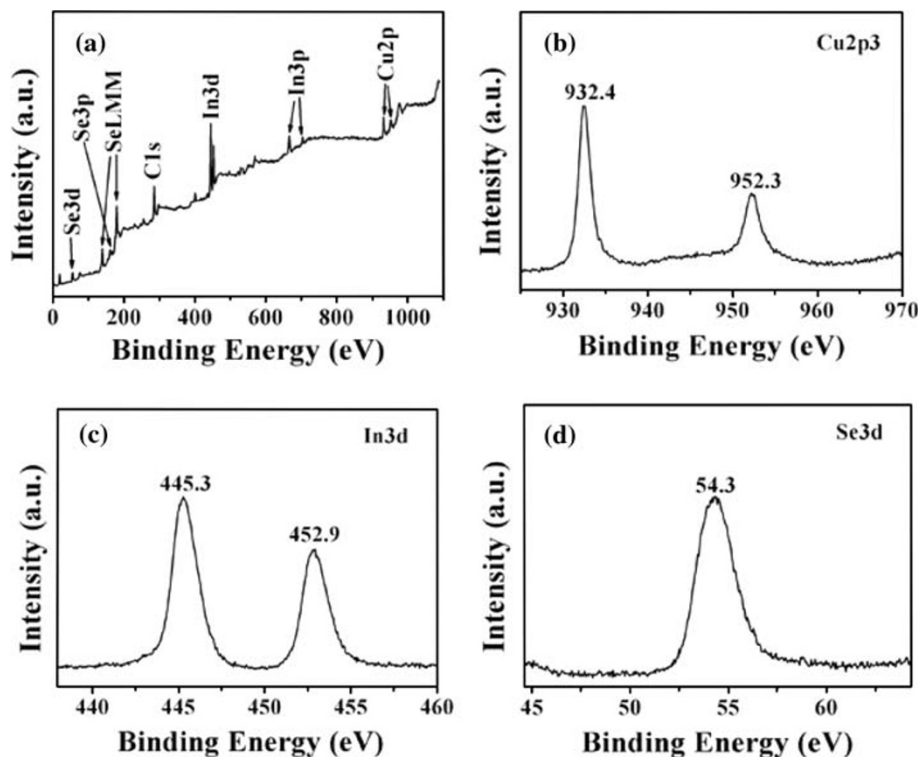
Fig. 2 (**a**) XPS survey spectrum, (**b**) Cu 2p, (**c**) In 3d, and (**d**) Se 3d core-level spectrum of the CuInSe$_2$ nanoparticles synthesized at 200 °C for 24 h

measured for the sample are $a = 0.577$ nm and $c = 1.162$ nm, which are in good agreement with the standard values of the reported data (JCPDS No.40-1487, $a = 0.578$ nm and $c = 1.162$ nm). Especially, the three-weak peaks including (211), (301), and (400) emerge here that distinguishes the chalcopyrite phase from the sphalerite phase. In addition, no peaks of other impurities were detected, indicating the high phase purity of CuInSe$_2$ sample.

Typical Raman spectrum of above CuInSe$_2$ sample was presented in Fig. 1b, where the most intense peak located at 173 cm^{-1} is attributed to A_1 mode because this is the strongest peak generally observed in the Raman spectrum of I-III-VI$_2$ chalcopyrite compounds. The A_1 mode in CuInSe$_2$ results from the motion of the Se atom, and the Cu and In atoms remain at rest. The other two weak peaks at 62 and 125 cm^{-1} can be assigned to B_2 and B_1 mode, respectively, and are well consistent with those reported for CuInSe$_2$ films. Besides, a shoulder peak characterizing the presence of Cu$_x$Se, which is usually centered at about 258 cm^{-1} [21], does not emerge in the Raman spectrum. The secondary phase Cu$_x$Se is always absent during the formation process of CuInSe$_2$ via the present approach, and the detailed reason will be discussed later.

The valence states of the elements in the above CuInSe$_2$ product were further investigated by XPS. The Cu 2p, In 3d, and Se 3d core levels were examined, respectively. The binding energies obtained in the XPS analysis were

corrected for specimen charging by referencing the C 1s to 284.6 eV. Figure 2a showed the XPS survey spectrum, and the Cu 2p core-level spectrum was illustrated in Fig. 2b. It was observed that two intense peaks were centered at 932.4 and 952.3 eV, corresponding to Cu 2p$_{3/2}$ and Cu 2p$_{1/2}$, respectively. The full widths at half maximum (FWHM) for peaks Cu 2p$_{3/2}$ and Cu 2p$_{1/2}$ were 1.9 and 2.3 eV, well consistent with the reported values for Cu$^+$ [22]. Furthermore, the binding energy for Cu^{2+} was usually located at 942 eV and emerged as a typical satellite peak [23], which was not observed in the present XPS spectrum. Hence, it can be concluded that the chemical valence of copper in the obtained product is +1 (Cu$^+$). Meanwhile, it can be clearly found from Fig. 2c that the peaks centered at binding energy of 445.3 and 452.9 eV coincided well with In 3d$_{5/2}$ and In 3d$_{3/2}$. The selenium 3d binding energy given by the core-level spectrum (Fig. 2d) was 54.3 eV. Both the In and Se 3d core-level spectra are very similar to those reported for CuInSe$_2$ [24].

The size and morphology of the CuInSe$_2$ synthesized at 200 °C for 24 h were investigated by scanning electron microscopy (SEM) and shown in Fig. 3a. The product is mainly composed of a large amount of nanoparticles with average size of about 80 nm, and these CuInSe$_2$ nanoparticles with irregular shapes were easily aggregated together. The size and microstructure of the product were further examined with transmission electron microscopy (TEM) and high-resolution TEM, respectively. From the
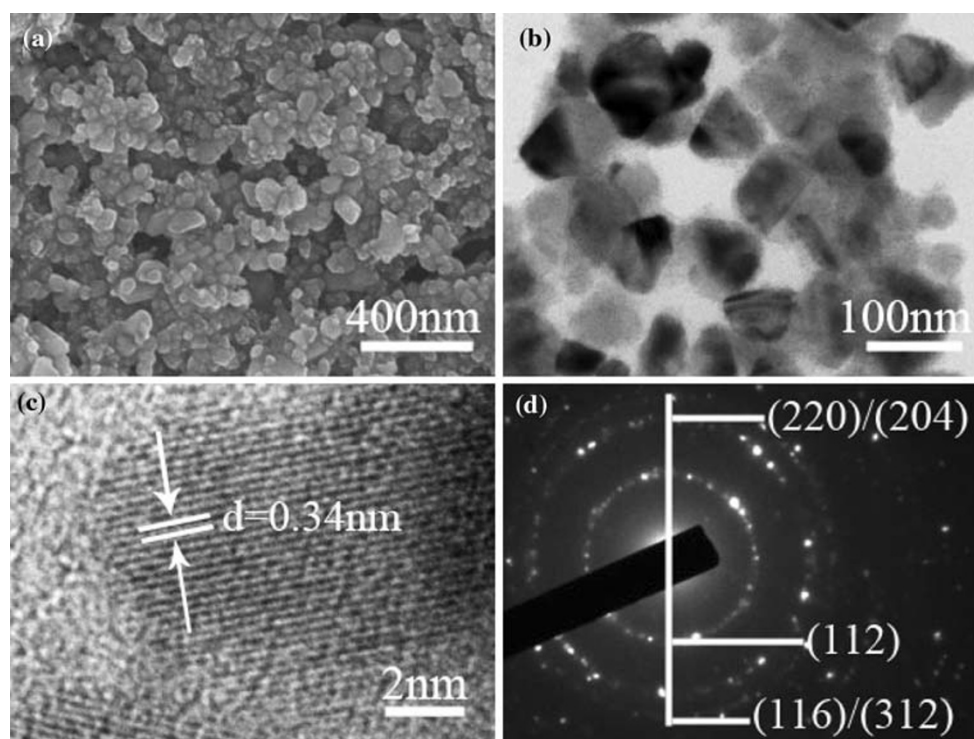
Fig. 3 SEM image (**a**) and TEM image (**b**) of CuInSe$_2$ nanoparticles prepared at 200 °C for 24 h. (**c**) HRTEM image and (**d**) The related SAED pattern of CuInSe$_2$ nanoparticles, the fringe spacing of 0.34 nm in (**c**) corresponds to (112) lattice planes

TEM image displayed in Fig. 3b, we can find that the CuInSe$_2$ nanoparticles still aggregated to some extent, although 20 min of sonication was employed in order to disperse it before the sample was deposited on the carbon-coated copper grid for the TEM measurement. The size is about 80–90 nm, almost consistent with that observed from SEM image. The HRTEM image of the nanoparticles is shown in Fig. 3c, where the lattice fringe is measured to be 0.34 nm corresponding to the (112) lattice plane of tetragonal CuInSe$_2$. The three ring selected area electrical diffraction (SAED) pattern shown in Fig. 3d corresponds to the (112), (220)/(204), (116)/(312) reflection direction of the tetragonal CuInSe$_2$. The SAED rings are not continuous but are composed of many discrete spots, not only suggesting the complex polycrystalline but also implying a preferential orientation of the collective CuInSe$_2$ nanoparticles.

To understand the influence of reaction time on the size of CuInSe$_2$ nanoparticles, several experiments were carried out on the basis of time variable, and the products obtained at different stages were investigated using the XRD and SEM techniques. From the XRD patterns shown in Fig. 4a, it can be found that the secondary phase of indium selenide binary compound exists with reaction less than 12 h when the temperature is fixed at 200 °C. There was no trace of second phase detected in the sample prepared for the

reaction time more than 15 h. After that, if longer time of solvothermal process was employed, the peaks belonging to the CuInSe$_2$ chalcopyrite phase were strengthened (e.g., 48 h), suggesting that the longer reaction time does favor the crystallization of the CuInSe$_2$ phase and high purity can be obtained. At room temperature, the elemental selenium can be dissolved in ethylenediamine gradually with the assistance of magnetic stirring, accompanied by the solution color changing from opaque to dark brown and the disappearance of selenium powder. In the following solvothermal stage, the reactivity of dissolved Se is greatly enhanced and it can be reduced to Se^{2-} by amine group. Meanwhile, the Cu$^+$ is chelated by bidentate ethylenediamine and forms the stable two-five-membered-ring chelated structure in which the Cu$^+$ bridges the amino groups of the two ethylenediamine moieties. Thus, the bidentate ligand complex effectively deters the formation of binary copper chalcogenides.

Figure 4b shows the SEM images of CuInSe$_2$ nanoparticles prepared with time of 15 h. Most of the nanoparticles have an average size of about 55–60 nm and only a few exceptions with larger grains coexist. With the reaction progressing to 24 h, the size would gradually grow into 80 nm, as shown in Fig. 3a. If we continued to increase the solvothermal treatment to 30 h while the temperature was still maintained at 200 °C, CuInSe$_2$ nanoparticles with

Fig. 4 (**a**) XRD patterns of CuInSe₂ products prepared at 200 °C for 12, 15, and 48 h. SEM images of CuInSe₂ nanostructures prepared 200 °C for (**b**) 15 h, (**c**) 30 h, and (**d**) 48 h
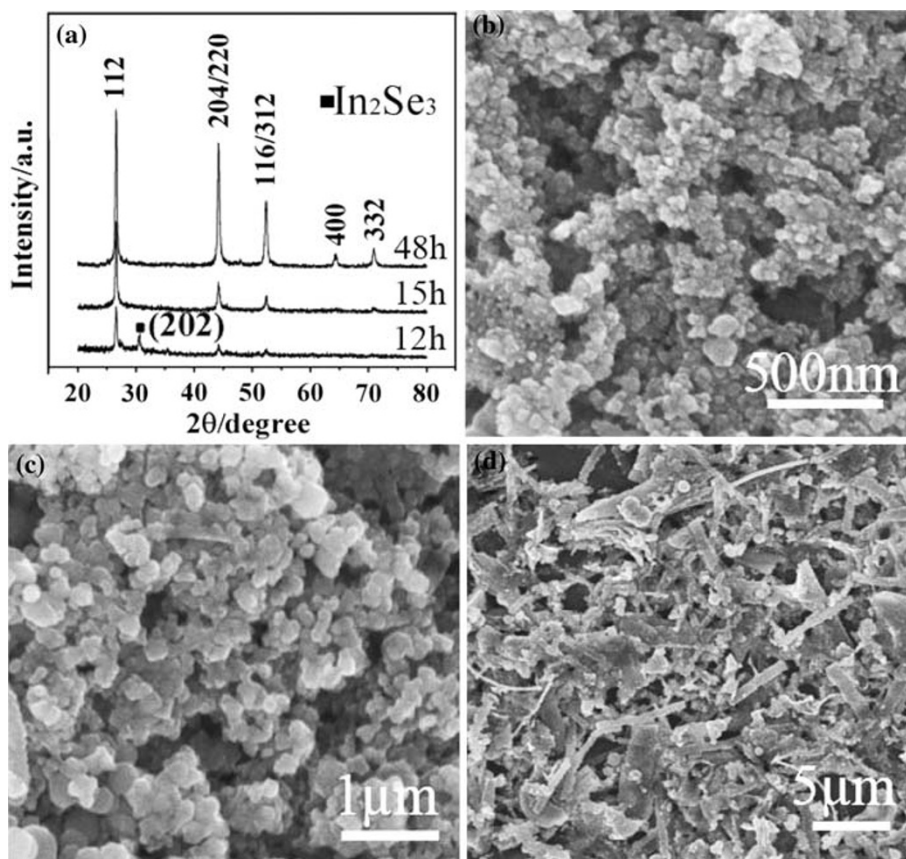
mean size of 200 nm were produced and still remained the irregular shapes (Fig. 4c). More complicated CuInSe₂ products including microspheres, rod- and belt-like structures were formed as the time was prolonged to 48 h (Fig. 4d). When the experiment was stopped at this stage, the reactant solution in the autoclave changed to light yellow, and the black products with microscale deposited on the bottom. Therefore, almost no CuInSe₂ within nanoscale could be collected by centrifugation from the solution.

The influence of temperature on the size of CuInSe₂ nanoparticles with a fixed reaction time of 24 h was also studied. When the temperature was reduced to 180 °C, the products mainly composed of small CuInSe₂ nanoparticles with the average diameters ranging from 40 to 50 nm, as revealed by the SEM image in Fig. 5a. The temperature effect was so distinct that a minute portion of binary compound would emerge in the final product when the temperature decreased to 160 °C, even the time was extended to 24 h. At lower temperature, less energy can be supplied and it is insufficient to complete the chemical reaction in a relatively short time. Thus, longer time was required in order to prepare CuInSe₂ nanoparticles with single pure phase at this temperature, which reversely resulted in the difficulty of controlling the size within a

definite range in nanoscale. In contrast, the product fabricated at 220 °C possesses the size in the range of 150–200 nm, as shown in Fig. 5b. Interestingly, the CuInSe₂ nanoparticles seem to be slightly fused each other on the surface instead of aggregated, and most of the interfaces between the nanoparticles were not clearly or fully observed. Sonication technique or rinsing several times with absolute ethanol was employed in an attempt to separate them, but it was not effective.

Generally, the magnitude of nanoparticles prepared via solution method can be controlled by some parameters such as reaction time, temperature, pH value, concentrations of precursors, solvent, and so on. However, when we attempted to control the size of CuInSe₂ nanoparticles by decreasing the concentrations of starting materials, the results are not satisfied. Figure 5c and d illustrate the SEM images of CuInSe₂ products synthesized at 200 °C for 24 h with the concentrations of half and one-third, respectively, compared to those in typical synthesis in the "Experimental" section. The size did not show obvious change and was almost in the range of 70–80 nm. Hydrothermal or solvothermal method has some advantages including low cost and convenience of handle. However, the disadvantage is also apparent that a relative long time is required to raise the temperature of solution
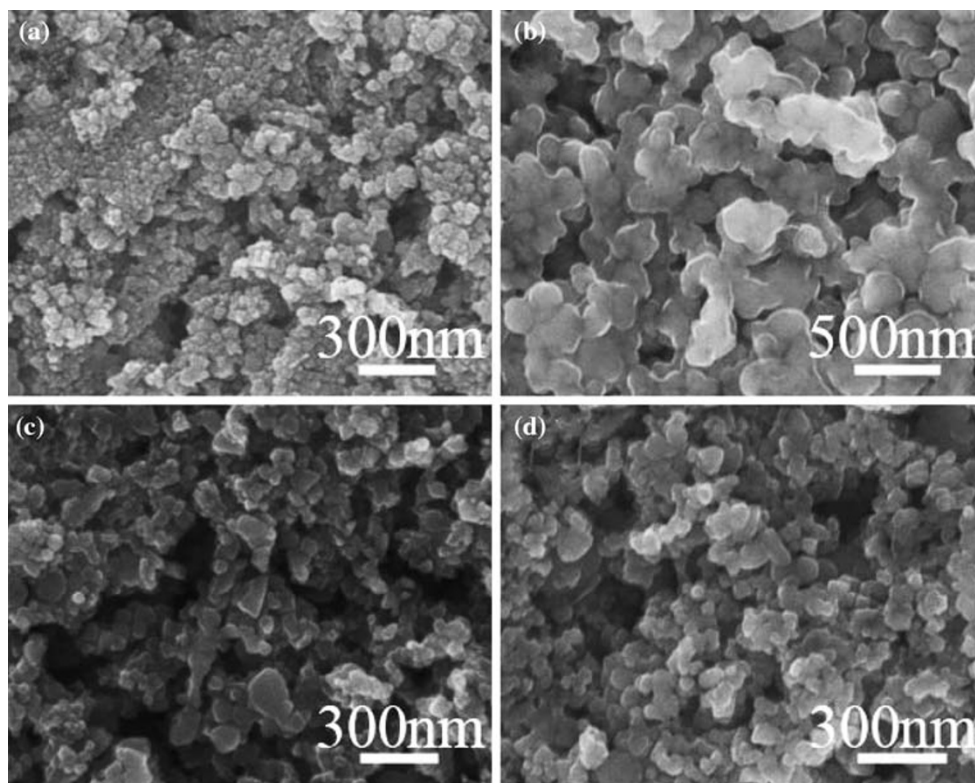
Fig. 5 SEM images of CuInSe$_2$ nanoparticles synthesized at (**a**) 180 °C and (**b**) 220 °C for 24 h, respectively. SEM images of CuInSe$_2$ nanoparticles prepared at 200 °C for 24 h with the concentration of starting materials decreased to that of half (**c**) and one-third (**d**) of the typical synthesis

in the autoclave to a target value, during which the reaction has already taken place and resulted in the difficulty in separating the nucleation stage from crystal growth step. Hence, the final nanoparticles are not expected to be uniform in both size and shape, as revealed by the previous SEM images. In the present work, in order to precisely control the size and phase of CuInSe$_2$ nanoparticles by simply changing some synthetic factors, further work should be carried out to understand the detailed mechanism and influences of preparation conditions, and some related research is currently in progress.

Figure 6 shows the UV–vis absorption spectrum of the CuInSe$_2$ nanoparticles prepared at 200 °C for solvothermal treatment of 15 h with ethylenediamine solvent. The sample was dispersed in absolute ethanol under intense sonication of 20 min and also ethanol was used as a reference. The result shows an absorption peak centered at approximately 440 nm. The band gap of the CuInSe$_2$ nanoparticles is calculated using the direct band gap method [16], and the value was determined to be 1.05 eV, which is consistent with the reported value of 1.04 eV for CuInSe$_2$ thin film [25]. Although the sample used for UV–vis absorption measurement is the one with the smallest size we can obtain at 200 °C through the present method, it
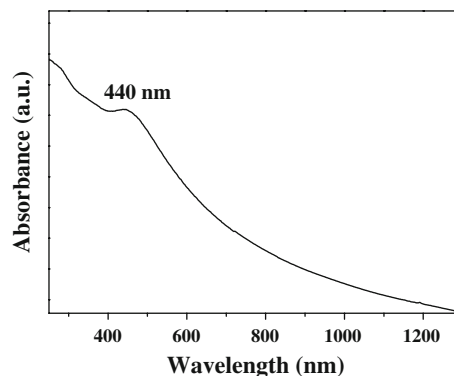

Fig. 6 The absorption spectrum of CuInSe$_2$ nanoparticles prepared at 200 °C for solvothermal treatment of 15 h

is still too large to observe the blue-shift due to quantum confinement effect.

Conclusions

In summary, the ternary I-III-VI$_2$ semiconductor of CuInSe$_2$ nanoparticles with controllable size has been successfully prepared via solvothermal approach. Elemental selenium powder, CuCl, and InCl$_3$ were used as starting

materials and ethylenediamine as solvent. The phase purity of the product can be easily controlled by varying reaction time at different temperatures, however, the optimal temperature for synthesizing $CuInSe_2$ nanoparticles within nanoscale ranges from 180 to 220 °C, only appropriate time of solvothermal treatment was employed. The as-obtained $CuInSe_2$ nanoparticles possess a band gap of 1.05 eV calculated from UV–vis spectrum. We believe these $CuInSe_2$ nanoparticles with controllable size could be processed into films and have wide potential applications in solar cell devices.

References

1. A. Rockett, R.W. Birkmire, J. Appl. Phys. **70**, R81 (1991). doi:10.1063/1.349175
2. C. Guillen, J. Herrero, Sol. Energy Mater. Sol. Cells **43**, 47 (1996). doi:10.1016/0927-0248(95)00163-8
3. V. Nadenau, D. Braunger, D. Hariskos, M. Kaiser, C. Koble, A. Oberacker, M. Ruckh, U. Ruhle, R. Schaffler, D. Schmid, T. Walter, S. Zweigart, H.W. Schock, Prog. Photovoltaics **3**, 363 (1995)
4. S. Niki, P.J. Fons, A. Yamada, T. Kurafuji, S. Chichibu, H. Nakanishi, W.G. Bi, C.W. Tu, Appl. Phys. Lett. **69**, 647 (1996). doi:10.1063/1.117793
5. J.A. Thornton, T.C. Lommasson, H. Talieh, B.H. Tseng, Sol. Cells **24**, 1 (1988). doi:10.1016/0379-6787(88)90030-0
6. A.M. Gabor, J.R. Tuttle, D.S. Albin, M.A. Contreras, R. Noufi, A.M. Hermann, Appl. Phys. Lett. **65**, 198 (1994). doi:10.1063/1.112670
7. J.F. Guillenmoles, A. Lusson, P. Cowache, S. Massaccesi, J. Vedel, D. Lincot, Adv. Mater. **6**, 376 (1994). doi:10.1002/adma.19940060507
8. J.F. Guillenmoles, P. Cowache, A. Lusson, K. Fezzaa, F. Boisivon, J. Vedel, D. Lincot, J. Appl. Phys. **79**, 7293 (1996). doi:10.1063/1.361446
9. S.L. Castro, S.G. Bailey, R.P. Raffaelle, K.K. Banger, A.F. Hepp, Chem. Mater. **15**, 3142 (2003). doi:10.1021/cm034161o
10. Y.H. Yang, Y.T. Chen, J. Phys. Chem. B **110**, 17370 (2006). doi:10.1021/jp062789r
11. B. Li, Y. Xie, J.X. Huang, Y.T. Qian, Adv. Mater. **11**, 1456 (1999)
12. Y. Jiang, Y. Wu, X. Mo, W.C. Yu, Y. Xie, Y.T. Qian, Inorg. Chem. **39**, 2964 (2000). doi:10.1021/ic000126x
13. M.G. Panthani, V. Akhavan, B. Goodfellow, J.P. Schmidtke, L. Dunn, A. Dodabalapur, P.F. Barbara, B.A. Korgel, J. Am. Chem. Soc. **130**, 16770 (2008). doi:10.1021/ja805845q
14. J. Tang, S. Hinds, S.O. Kelley, E.H. Sargent, Chem. Mater. **20**, 6906 (2008). doi:10.1021/cm801655w
15. X.L. Gou, F.Y. Cheng, Y.H. Shi, L. Zhang, S.J. Peng, J. Chen, P.W. Shen, J. Am. Chem. Soc. **128**, 7222 (2006). doi:10.1021/ja0580845
16. Q. Guo, S.J. Kim, M. Kar, W.N. Shafarman, R.W. Birkmire, E.A. Stach, R. Agrawal, H.W. Hillhouse, Nano Lett. **8**, 2982 (2008). doi:10.1021/nl802042g
17. B. Koo, R.N. Patel, B.A. Korgel, J. Am. Chem. Soc. **131**, 3134 (2009). doi:10.1021/ja8080605
18. H.Z. Zhong, Y.C. Li, M.F. Ye, Z.Z. Zhu, Y. Zhou, C.H. Yang, Y.F. Li, Nanotechnology **18**, 025602 (2007). doi:10.1088/0957-4484/18/2/025602
19. C. Burda, X. Chen, R. Narayanan, M.A. El-Sayed, Chem. Rev. **105**, 1025 (2005). doi:10.1021/cr030063a
20. H. Matsushita, T. Takizawa, J. Cryst. Growth **179**, 503 (1997). doi:10.1016/S0022-0248(97)00147-4
21. P.F. Luo, C.F. Zhu, G.S. Jiang, Solid State Commun. **146**, 57 (2008). doi:10.1016/j.ssc.2008.01.020
22. J. Llanos, A. Buljan, C. Mujica, R. Ramirez, J. Alloys Compd. **234**, 40 (1996). doi:10.1016/0925-8388(95)02062-4
23. L.D. Partain, R.A. Schneider, L.F. Donaghey, P.S. Mcleod, J. Appl. Phys. **57**, 5056 (1985). doi:10.1063/1.335283
24. K. Bindu, C. Sudha Kartha, K.P. Vijayakumar, T. Abe, Y. Kashiwaba, Sol. Energy Mater. Sol. Cells **79**, 67 (2003). doi:10.1016/S0927-0248(02)00367-7
25. H.S. Soliman, M.M. El-Nahas, O. Jamjoum, Kh.A. Mady, J. Mater. Sci. **23**, 4071 (1988)